Aligned Nano-Porous Microwave Exfoliated Graphite Oxide Ionic Actuators with High Strain and Elastic Energy Density

*M. Ghaffari, W. Kinsman, Y. Zhou, S. Murali, Q. Burlingame, M. Lin, R. S. Ruoff, and Q. M. Zhang**

Materials that can generate large actuation with a high force level under external electrical signals are of great importance for applications such as artificial muscles, precise motion and position control, and micro-electromechanical systems.[1–9] It is especially appealing if the large electro-actuation strain can be induced and controlled by a few volts, since this may lead to direct integration of these micro-actuators with advanced micro-electronics to perform complex functions which are not possible with existing actuators and actuation mechanisms.[1,4,5,7–12] The observation of the very large electro-actuation strains (> 50%) in a class of dielectric elastomers with an elastic energy density > 1 J cc^{-1} in 2000 attracted a great deal of attention for this reason.[3] The very high voltage (> 1000 V) required to induce such a high strain as well as the low elastic modulus of the dielectric elastomers (≈1 MPa), however, limited their applications. On the other hand, ionic polymer actuators such as gels and soft polymers that contain a high fraction of water can generate strains > 50% under a few volts. Nevertheless, a major constraint of these gel actuators for practical applications is their extremely low elastic modulus (< 1 MPa).[13–15]

Graphene, as a single atomic layer sheet conductor with high mechanical strength and electric conductivity, represents perhaps an ideal material system for ionic actuators to achieve high strain with high elastic energy density induced electrically at low voltages. Although the graphene-based electromechanical actuator devices studied so far possess very limited strain,[16–18] we show in this paper that a class of aligned activated "nano-porous" microwave exfoliated graphite oxide (A-aMEGO) actuators with controlled nano-morphology can generate an electro-actuation strain of more than 50% with a high force generating capability, as measured by the large elastic energy density (≈1.5 J cc^{-1}) under a few volt electrical excitation. Another unique feature of the nano-porous A-aMEGO actuators developed in this paper is the large anisotropy of the electro-actuation strain generated, resulting from the nano-morphology of the high degree of alignment (orientation) of the nano-pores. Namely, the large strain is induced along the direction of the average surface normal to the graphene sheets (see **Figures 1**a and 1b) while in the directions perpendicular to that, the strain is negligible. Such a large strain anisotropy is highly desired for most practical applications as will be discussed in the following sections.

The basic actuation principle of the A-aMEGO actuators to be developed in this paper is schematically illustrated in Figure 1a, where the ingression and/or depletion of mobile ions in the nano-pores, in order to compensate the changes in electronic charges on the A-aMEGO electrodes under external voltage, will cause changes in the inter-sheet spacing. If the distance between the adjacent graphene walls is comparable to the change of this inter-sheet space, a large strain (>50%) can be generated. Recently, Zhu et al. reported the activation of MEGO with KOH where a Brunauer-Emmett-Teller (BET) specific surface area (SSA) of 3100 m^2g^{-1} can be achieved and because the nano-pore inter-wall space size is between 1 nm and 4 nm, the new graphene material was named activated microwave exfoliated graphite oxide (aMEGO).[19] Thus, if the aMEGO sheets can be properly assembled, these graphene-based ionic devices have the potential to achieve giant electro-actuation strain induced under a few volts.

For A-aMEGO actuators, the electro-actuation strain illustrated in Figure 1a is predominantly along the direction perpendicular to the sheet surface. Hence, the ionic actuator device should have the nano-morphology of aligned (highly oriented) nano-porous aMEGO in order to translate the atomic layer actuation in Figure 1a into the largest linear electro-actuation in an ionic device, as schematically

M. Ghaffari, W. Kinsman
Department of Materials Science and Engineering
Materials Research Institute
The Pennsylvania State University
University Park, PA, 16802, USA

Y. Zhou, Q. Burlingame
Department of Electrical Engineering
Materials Research Institute
The Pennsylvania State University
University Park, PA, 16802, USA

S. Murali, Prof. R. S. Ruoff
Department of Mechanical Engineering and Materials Science and Engineering Program
University of Texas at Austin
One University Station, C2200, Austin, TX, 78712, USA

Dr. M. Lin
Materials Research Institute
The Pennsylvania State University
University Park, PA, 16802, USA

Prof. Q. M. Zhang
Department of Electrical Engineering
Department of Materials Science and Engineering
Materials Research Institute
The Pennsylvania State University
University Park, PA, 16802, USA
E-mail: Qxz1@psu.edu

Prof. Q. M. Zhang
School of Materials Science and Engineering
Tsinghua University
Beijing, 100084, P. R. China

DOI: 10.1002/adma.201301370

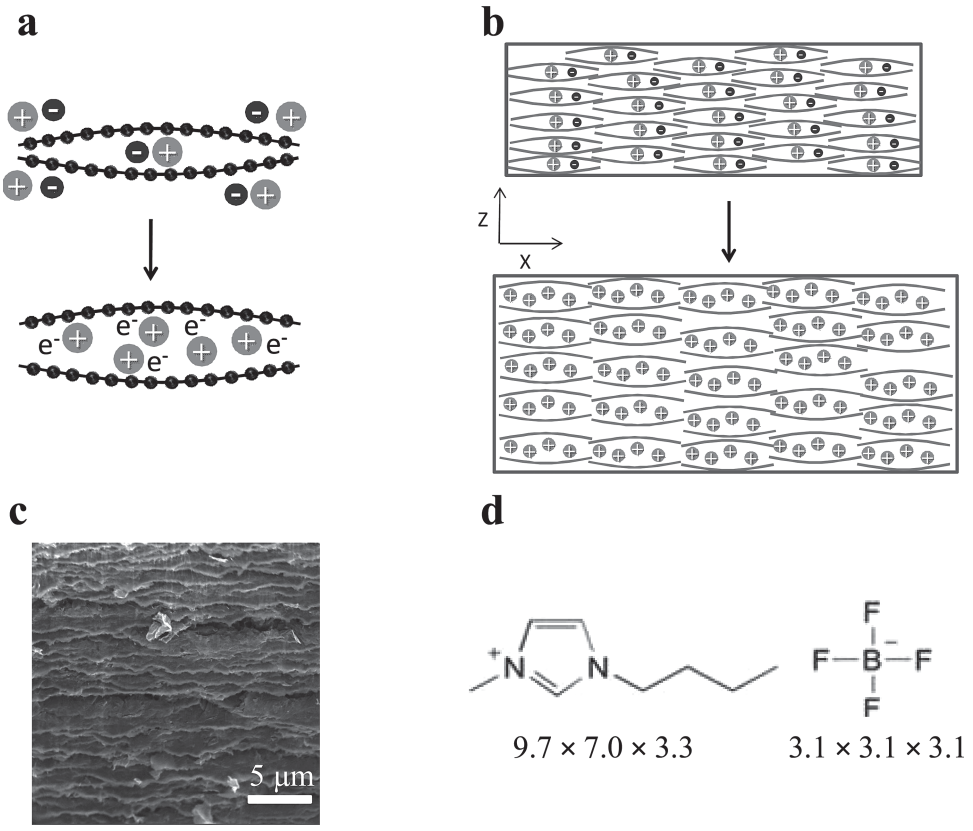

Figure 1. (a) An illustration of ionic electro-actuation in graphene sheets where the ingression of the mobile ions (blue circles, cations here) into the interlayer space upon the application of an external voltage generates large strain when the interlayer spaces are comparable to the mobile ion sizes. e^- represents the electron charges on the cathode (graphene sheets). (b) Schematic of the nano-morphology of highly oriented aMEGO sheets of an ionic actuator employing the actuation mechanism in (a), generating large electro-actuation strain along the z-direction ('thickness direction'). (c) SEM image of A-aMEGO samples. (d) The chemical structure and dimensions (in Å) of $BMIM^+$ and BF_4^- ions.[26]

shown in Figure 1b. To realize that, a vacuum-assisted self-assembly process was employed, which can produce highly aligned aMEGO sheets in device sizes from several microns to macroscopic sizes (Figures S1a and S1b, Supporting Information).[20–23] In this study, packed A-aMEGO samples of several millimeter lateral sizes and up to 0.05 mm thickness were fabricated. As shown by the SEM image in Figure 1c, the A-aMEGO samples thus fabricated indeed have highly aligned nano-morphology. The dry A-aMEGO sheets fabricated into such films have a density of 1.25 g cm^{-3}. Comparison with the density of graphite (2.2 g cm^{-3}) indicates that the films comprised of such A-aMEGO sheets have a pore volume fraction of 43%.

For the ionic A-aMEGO/polymer nano-composite actuators, two polymer binders were investigated; the traditional poly(tetrafluoroethylene) (PTFE) which is widely used for fabricating supercapacitor electrodes and has a dielectric constant of 2.1 and a polar fluoropolymer poly(vinylidene fluoride/chlorotrifluoroethylene) (P(VDF-CTFE) 91/9 mol% composition) which has a high dielectric constant of 12.[11,24,25] The high dielectric constant binders may improve the mobile ion concentration in the nano-composite electrodes, resulting in higher capacitance values and hence higher ion concentrations accumulated in these electrodes.[24]

For ionic electroactive actuators, electrolytes play a critical role by providing mobile ions for the actuations as illustrated in Figures 1a and 1b.[4–7,10] In this study, an ionic liquid (IL)/molecular liquid (ML) mixture was used as the electrolyte. An imidazolium based IL, 1-butyl-3-methylimidazolium tetrafluoroborate ([BMIM][BF_4]) whose chemical structure and dimensions are presented in Figure 1d, was selected as the IL.[26] Imidazolium based ILs have been studied widely for ionic electroactive devices because of their high ionic conductivity and large electrochemical window.[4,7,27] Acetonitrile (AN) was used as the ML in this study. Many studies have shown that a proper IL/ML mixture can improve the ionic conductivity and mobility markedly compared with a pure IL.[27] In addition to the pure IL, the nano-composites were directly soaked in the 2M [BMIM][BF_4]/AN electrolyte which resulted in a 60–62 wt% of electrolyte in the final composite.

The electro-actuation strains in both the cathode and anode of the ionic A-aMEGO/polymer nano-composites were characterized in a configuration as illustrated in Figure S2. **Figure 2**a presents the cyclic electro-actuation thickness strain (along the z-direction of Figure 1b) of the A-aMEGO/P(VDF-CTFE) with [BMIM][BF_4]/AN electrolyte under a peak voltage of 4 V at a 50 mV s^{-1} scan rate, measured at the cathode. Electro-actuation strain of the actuators is calculated using Equation (1) as:

Adv. Mater. **2013**,
DOI: 10.1002/adma.201301370

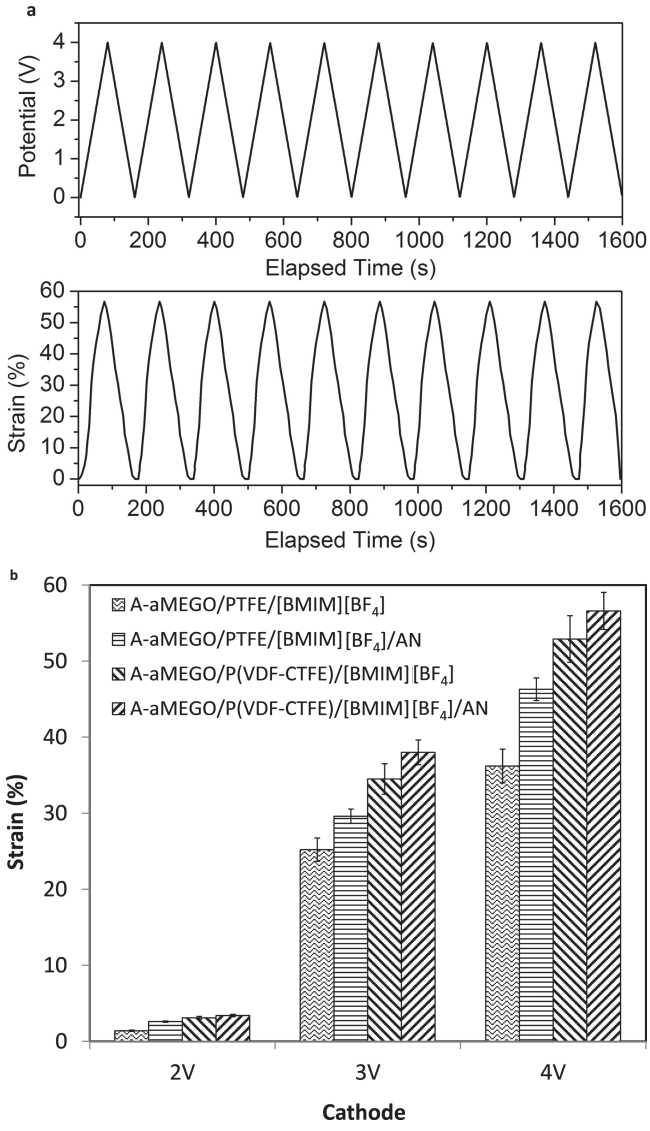

Figure 2. (a) Applied voltage between the cathode and anode (top) and electro-actuation strain of the cathode versus time (bottom) for the A-aMEGO/P(VDF-CTFE) nano-composites with [BMIM][BF_4]/AN at 50 mV s^{-1} scan rate. The strain shows a near linear response with the applied voltage. (b) Electro-actuation strain on the cathode for the A-aMEGO/polymer nano-composites investigated at different applied peak voltages and 50 mV s^{-1} scan rate. The error bars are also indicated in the figure.

$$Strain = \left(\frac{Final\ Thickness - Initial\ Thickness}{Initial\ Thickness}\right) \times 100 \qquad (1)$$

The strain value increases almost linearly with the voltage and reaches the maximum value of 56.6% at 4 V. The electro-actuation strains perpendicular to the thickness direction were also characterized using an optical microscope, and showed strain values less than 3%, which is more than 18 times smaller than those along the thickness direction, and has a sign opposite that of the thickness strain. Similar trends were also observed for all the nano-composites investigated at different peak voltages (from 2 V to 4 V). Such large electro-actuation strain anisotropy is caused by the unique nano-morphology of the highly oriented nano-pores of the aMEGO sheets, as illustrated in Figure 1b. Electromechanical actuators with such large strain anisotropy are highly desirable for practical applications. Most practical electromechanical applications in fact use electro-actuation strains along a single direction and the electro-actuation strains induced in the perpendicular directions often create adverse effects which reduce the actuator performance.[28,29]

Figure 2b summarizes the peak values of the electro-actuation thickness strain on the cathode side of the A-aMEGO/P(VDF-CTFE) as well as A-aMEGO/PTFE nano-composites at several peak voltages with a scan rate of 50 mV s^{-1} using the IL/ML electrolyte as well as the pure IL. The A-aMEGO/P(VDF-CTFE) nano-composites with IL/ML exhibit the highest strain value of 56.6% while A-aMEGO/PTFE with pure IL shows the lowest strain value of 36.2% at voltages less than 4 V, which is still quite large. The results also show that the nano-composites with IL/ML electrolytes generate higher strain compared to those with pure IL. The higher ionic mobility of the IL/ML electrolyte is responsible for the higher strain since for a fixed scan rate, a higher ionic mobility will cause a higher excess mobile ion concentration in the nano-porous electrodes.

The capacitance of the ionic A-aMEGO/polymer nano-composite actuators was measured with a potentionstat and the cylic voltammetry (CV) curves at different scan rates for A-aMEGO/PTFE sample with [BMIM][BF_4]/AN is shown in Figure S3 as an example. The CV curves for these samples are nearly rectangular which is an indication of non-Faradic charge transfer in A-aMEGO-based electrodes. The specific capacitance for the ionic A-aMEGO/P(VDF-CTFE) with [BMIM][BF_4]/AN electrolyte nano-composites, deduced from CV cruves, was 192 F g^{-1} at a 4 V peak voltage and a 50 mV s^{-1} scan rate, which is consistent with earlier studies of supercapacitors based on nano-porous aMEGO.[19] The results indicate that the nano-composite thus fabricated possesses very large electrode/electrolyte interfacial area and the graphene sheets in the nano-composite are mostly in the single atomic sheet-form. The large specific electrode area coupled with the high degree of alignment of the aMEGO flakes in the nano-composite leads to the generation of the giant electro-actuation in the nano-composites along the thickness direction. The specific capacitances of A-aMEGO/P(VDF-CTFE) with pure [BMIM][BF_4] electrolyte, A-aMEGO/PTFE with [BMIM][BF_4]/AN electrolyte, and A-aMEGO/PTFE with pure [BMIM][BF_4] electrolyte are also presented in **Figure 3**a. The specific capacitances of A-aMEGO/P(VDF-CTFE) nano-composites are larger than that of A-aMEGO/PTFE. Consistent with earlier experimental results, the specific capacitance of the nano-composites with the IL/ML electrolyte is higher than that with the pure IL due to the increased mobile ion concentration and high ionic conductivity in IL/ML solutions.[27]

Figure 3b presents the ratio of the electro-actuation strain on the cathode over specific capacitance at different voltages and a 50 mV s^{-1} scan rate for the prepared nano-composites. The results show that the ionic A-aMEGO/polymer nano-composite with higher specific capacitance also exhibits a higher electro-actuation strain. These results also indicate that the strain response of this class of newly developed ionic A-aMEGO/polymer nano-composites is sensitive to the properties of constituents and electrolytes. A higher strain response might be

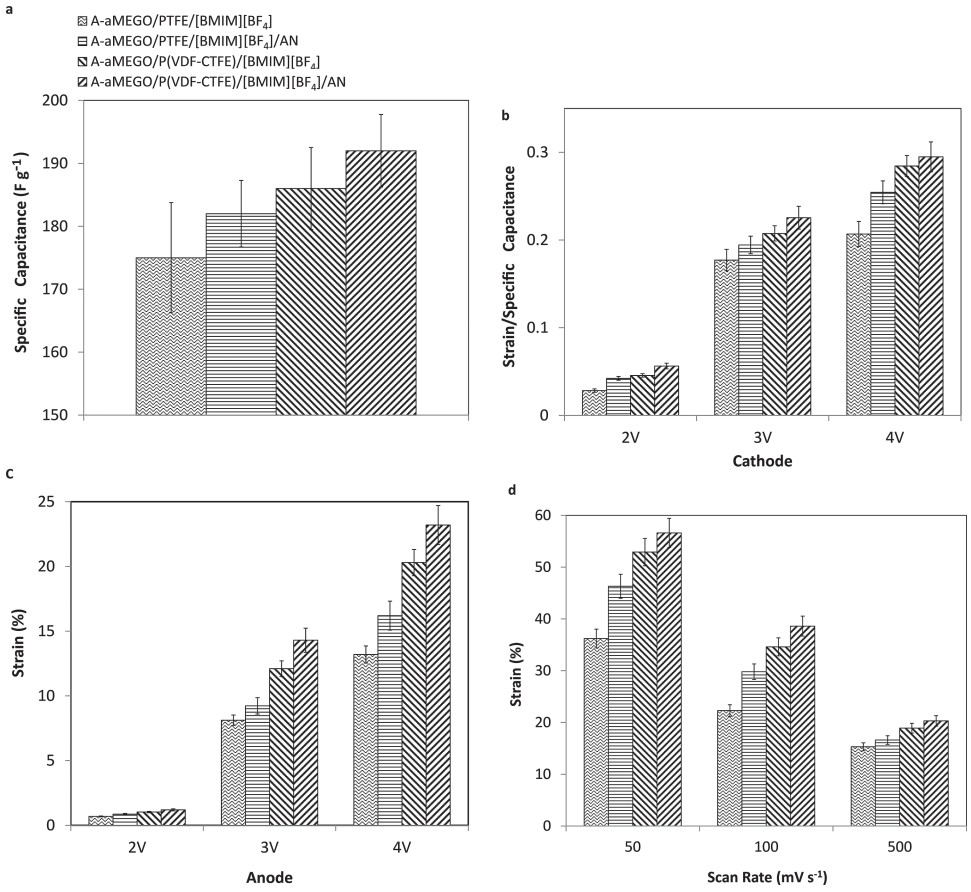

Figure 3. (a) Specific capacitances of the ionic A-aMEGO/polymer nano-composites determined from the cyclic voltammetry at 4 V peak voltage and 50 mV s^{-1} scan rate. (b) The ratio of the strain over specific capacitance at different voltages and 50 mV s^{-1} scan rate. (c) Electro-actuation strain on the anode side for the A-aMEGO/polymer nano-composites investigated at different applied peak voltages and 50 mV s^{-1} scan rate. (d) Strain at 4 V peak voltage of the cathode at different scan rates. The error bars are shown in all figures. The legends are the same for all four figures.

obtained by further tailoring material parameters in the nano-composites. Nevertheless, these experimental results have already demonstrated an exceptionally high electro-actuation strain generated at voltages less than 4 volts.

The electro-actuation strain on the anode side was also characterized as represented in Figure 3c, which is positive but much smaller than that on the cathode side. The difference in the strain values between the cathode and the anode might be caused by different sizes of the cation and anion (the cation's volume is about 3 times larger than that of the anion) in the electrolytes.[30,31] A recent direct observation using Time-of-Flight Secondary Ion Mass Spectrometry (TOF-SIMS) in the ionic polymer nano-composite membrane actuators with 1-butyl-2,3-dimethylimidazolium chloride (BMIM-Cl) as the electrolyte, also showed similar behavior where both cathode and anode electrodes exhibited positive strains.[32] The anode, due to the smaller size of the anions, exhibited much smaller strain compared with that at the cathode.[32] The results indicate that by varying the size of cations and anions in ILs, the strain level at the two electrodes can be tailored.

The actuator responses at higher frequencies (100 mV s^{-1} and 500 mV s^{-1} scan rates) under 4 V were also characterized and presented in Figure 3d. As expected for ionic devices such as supercapacitors and ionic actuators, increasing operation frequency reduces the capacitance of supercapacitors and the actuation strain in ionic actuators. Even so, when increasing the scan rate from 50 mV s^{-1} to 500 mV s^{-1} the strain for the A-aMEGO/P(VDF-CTFE) with IL/ML electrolyte is still 20.3% under 4 volts. Since the operation frequency of these ionic actuators is limited by the net time for the mobile ions to enter and leave the nano-composite electrodes, one can increase the operation frequency while maintaining high strain response by reducing the path length for the mobile ions to travel in the electrodes.[7,24,25] For the A-aMEGO/polymer nano-composites here, this means a reduction of the actuator lateral dimension (along the x-directon in Figure 1 which forms the aligned mobile ion transport pathways). Since the mobile ion transport in the nano-porous electrodes is through both the drifting (the time constant is proportional to the distance) and diffusion (the time constant is proportional to the square of the ion transport distance), by reducing the actuator lateral dimension, for example, from the current 2 mm to smaller values such as 0.1 mm, will result in a more than 20 times improvement in the actuator speed.

In addition, the strain rates as functions of applied voltage and scan rate at the cathode are summerized in Figure S4. As shown, in the voltage range measured (<4 V) the strain

Adv. Mater. 2013,
DOI: 10.1002/adma.201301370

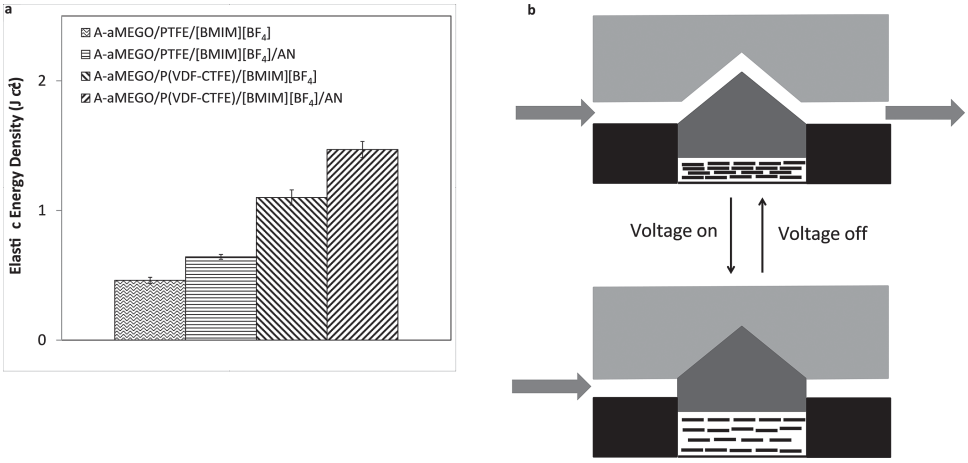

Figure 4. (a) Elastic energy density of the ionic A-aMEGO/polymer nano-composites at 4 V and 50 mV s^{-1} scan rate. Error bars are indicated in the figure. (b) Schematic of a micro-valve constructed using the cathode of the A-aMEGO actuator where the arrows indicate the flow direction. With a 0.1 mm thick cathode, a strain of >50% in the cathode will generate a 50 µm displacement to close the flow. The anode and the gel electrolytes are not shown in the figure.

rate increases with the applied voltage and scan rate. At 4 V and 500 mVs^{-1} scan rate, a 2.54% s^{-1} can be obtained for the A-aMEGO/P(VDF-CTFE) nano-composite actuator with IL/ML as electrolyte.

Besides the electro-actuation strain, the ability to generate stress is another critical parameter for actuators. The elastic energy density is used to characterize an actuator material's strain and stress generation capability.[1–3,33] Following Hooke's law, the stress generated is proportional to the elastic modulus of the actuator material. The elastic modulus Y of the A-aMEGO/polymer nano-composites with the electrolytes swelled along the z-direction (see Figure 1b) when the composite actuators were not charged (under no voltage) was characterized by an AFM using a tapping method[34,35] (see Supporting Information) and a value of 67.5 ± 12.5 MPa was obtained. This elastic modulus value is similar to the other ionic polymer actuators swelled with electrolytes in previous studies.[7,36] The elastic modulus of the composite actuators under applied voltage was also characterized by measuring the induced strain under different mechanical stress (see Figure S5). The elastic modulus was reduced to 9 MPa at 56.6% strain (under 4 V) for the A-aMEGO/P(VDF-CTFE) nano-composites with IL/ML electrolyte, which is still quite high. Such a high elastic modulus coupled with the high electro-actuation strain generates a high elastic energy density.[1–3]

Because of the high strain level, the elastic energy density U_m is derived from the mechanical energy generated divided by the actuator volume [2,34,37]

$$U_m = \int_{l_0}^{l} Y \ln(x) dx \quad (2)$$

where $x = l/l_0$, l_0 is the initial composite thickness and l is the thickness after the electro-actuation (see Supporting Information). The initial nano-composite volume ($Vol = A \times l_0$) is used in calculating the elastic energy density in Equation (2) where the area A does not change with the voltage due to the large elastic anisotropy of the A-aMEGO/polymer nano-composites. Here, the change in elastic modulus by strain was taken into consideration in Equation (2). The elastic energy densities calculated for various A-aMEGO/polymer nano-composites investigated at 4 V and 50 mV s^{-1} scan rate are summarized in **Figure 4**a which are in the range of 0.5 – 1.5 J cc^{-1} for different samples. These values are among the highest for ionic actuators performing under voltages lower than 4 V. **Table 1** compares the A-aMEGO/P(VDF-CTFE) with [BMIM][BF_4]/AN as the electrolyte with several high performance ionic electroactive polymers (with high electro-actuation strains) reported in the literature, which shows the high strain and high elastic energy density of this newly developed actuator materials.[3,11,38–43] In the Table, the high strain dielectric elastomers are also included, which require very high voltage (> 1000 volts) and high electric fields (> 200 MV m^{-1}) to induce high strains with the elastic energy density comparable to the A-aMEGO nano-composite actuators

Table 1. Comparison of the strain, elastic modulus, elastic energy density and applied voltage for A-aMEGO/P(VDF-CTFE) actuators with high performance electroactive systems reported in the literature.

Material	Strain (%)	Elastic Modulus (MPa)	Elastic Energy Density (J cc^{-1})	Applied Voltage (V)
aMEGO/P(VDF-CTFE)	56.6	9.0 – 67.5	1.5	4
Polypyrrole[39]	35	-*	–	1
Polypyrrole[40]	34	6.7	–	0.9
Meso-carbon microbeads[42]	40	–	–	5.0
Polyaniline[43]	20	–	-	0.4
Silicone[3,11]	120	0.1 – 1.0	<1.0	> 1,000 (350 MV m^{-1})
Acrylic [3,11]	380	1.0	3.4	> 1,000 (440 MV m^{-1})

*: data not reported.

reported here.[3,11] Some of these high performance actuators have anisotropic properties similar to the actuator system reported herein.[39,41] The high performance features of the A-aMEGO actuators render them potentially valuable systems for micro-electromechanical systems (MEMS) applications such as micro-values, as illustrated in Figure 4b.

In conclusion, making use of the nano-porous aMEGO with highly anisotropic nano-pores and single atomic sheet graphene walls which possess high electronic conductivity and high mechanical strength, this work demonstrates a new class of A-aMEGO/polymer nano-composite based actuators that can exhibit higher than 50% electro-actuation strain with an elastic energy density > 1 J cc^{-1}. Unique nano-morphology of A-aMEGO actuators leads to a large anisotropy in the electro-actuation strains, which is highly desired for most electromechanical applications. These A-aMEGO/polymer nano-composite actuators can be fabricated using the self-assembly method in both the micro-scale and macro-scale, making them suitable for applications over a broad length scale. Also, the unique anisotropic features of the proposed actuator system make them useful for applications requiring unidirectional force and displacement, as demonstrated in Figure S6. These attractive features, plus the low operation voltage, provide an opportunity for direct integration of these micro-actuators with advanced micro-electronics, which may expand the device paradigms beyond the reach and functionality of traditional actuators and micro-electronics.

Experimental Section

A-aMEGO fabrication: The synthesis of what we here refer to as 'nano-porous aMEGO' has been presented in detail in Ref. [19]. We used a vacuum-assisted self-assembly method to fabricate the highly aligned nano-porous aMEGO sheets (as well as A-aMEGO/P(VDF-CTFE) nano-composites).[20–23] To fabricate highly aligned aMEGO, nano-porous aMEGO (10 mg) was dispersed in N,N-dimethylformamide (DMF, Aldrich, 5 ml). Next, this mixture was vacuum filtered using a Buchner funnel and an Anodisc filter membrane (Whatman, 0.02 μm pore size) in order to align aMEGO sheets, as illustrated in Figure S1a. Finally, the oriented nano-porous aMEGO disk was air dried for 2 hours and vacuum dried in air at 70 °C for 1 hour. As illustrated in Figure S1a, the alignment process takes place by a uniform capillary force imposed by vacuum through the pores in the Anodisc membrane. During this filtration process, nano-porous aMEGO layers are pulled towards the Anodisc surface and these layers of nano-porous aMEGO stack successively on top of each other as shown in the SEM image of Figure 1c.

A-aMEGO/PTFE nano-composite fabrication: In order to prepare a nano-composite containing 10 wt% PTFE (Aldrich) as a binder and 90 wt% A-aMEGO as the matrix, a commercially available 60 wt% dispersion of PTFE in water was diluted by isopropyl alcohol and used. The A-aMEGO disk was placed in a petri dish containing the PTFE dispersion (with 10 wt% of PTFE). In order to allow PTFE polymer chains enough time to penetrate through nano-porous aMEGO sheets and make a uniform composite, different exposure times were evaluated using a well-controlled evaporation rate chamber. It was found that after a slow water/isopropyl alcohol evaporation over one week, homogeneous well aligned nano-porous aMEGO/PTFE nano-composites were formed, which were then annealed at 140 °C and kept in a dry box for further testing. The volume content of the PTFE binder in the nano-composites can be tailored by varying the amount of PTFE infiltrated into A-aMEGO.

A-aMEGO/P(VDF-CTFE) nano-composite fabrication: A one-step vacuum-assisted self-assembly approach was directly used to prepare P(VDF-CTFE)-based nano-composite. First, a solution of P(VDF-CTFE) (Solvey, Solef 31508) in DMF (0.2 wt%) was prepared along with a dispersion of aMEGO (10 mg) in DMF (2 mL). Then the P(VDF-CTFE) solution and aMEGO dispersion were mixed together in a 1:1 ratio and sonicated for half an hour to ensure a uniform dispersion. The mixture was then filtered through an Anodisc similar to the previous example. Finally, the obtained disk was dried and annealed at 140 °C. Weight measurements indicated that the weight ratio of A-aMEGO to P(VDF-CTFE) was 9/1. This process is shown in Figure S1b. The volume content of P(VDF-CTFE) in the nano-composites can be varied by changing the ratio of the solution of P(VDF-CTFE) *vs.* aMEGO dispersion.

Ionic liquid infiltration: To fabricate the ionic actuators, the A-aMEGO/polymer composites were swelled by a properly selected electrolyte (that was thus absorbed into the composite). Both the pure room temperature IL of [BMIM][BF_4] (Iolitec) and its 2M solution in acetonitrile ([BMIM][BF_4]/AN) were used as electrolytes in this study. Square shaped A-aMEGO/PTFE or A-aMEGO/P(VDF-CTFE) (50 micron thick) were cut and placed in an electrolyte bath at room temperature. After the nano-composites were completely infiltrated by the electrolyte (≈30 minutes), they were used for electro-actuation as well as cyclic voltammetry characterizations. Figure S1c schematically shows the infiltration of PTFE and [BMIM][BF_4] into A-aMEGO. It was observed that the thickness of the nano-composite increased by 25% (along the z-direction in Figure 1b) while the change in the lateral dimension was less than 3% (perpendicular to the z-direction in Figure 1b). The observed large elastic anisotropy was caused by the nano-morphology of the highly oriented aMEGO sheets in the composites.

Characterization of the electro-actuation: The electro-actuation strain in the ionic A-aMEGO/polymer nano-composites was characterized in a configuration as illustrated in Figure S2. Two A-aMEGO/PTEF or A-aMEGO/P(VDF-CTFE) nano-composites of 2 mm × 2 mm lateral size and 0.05 mm thick (along the z-direction) were bonded to the bottom of a Teflon sample holder filled with [BMIM][BF_4]/AN electrolyte which has two square shaped dishes of 3 mm diameter and 1 mm depth connected by a 1 mm wide channel for the ion conduction between the two nano-composite electrodes. The two nano-composites served as two electrodes and two stainless steel (SS) pins with flat heads of 1.5 mm diameter were used as the current collectors, which were pressed lightly to the top surfaces of the two nano-composites. The positions (both lateral and vertical) of the SS electrodes were precisely controlled by micro-manipulators. The electro-actuation strains in both the cathode and anode were characterized using a fiber optic displacement sensor (MTI 2100 Fotonic) which has a resolution of 25 nm. A small (2 mm × 2 mm × 0.1 mm) aluminum plate was glued to one of the electrodes to serve as a diffuse reflection surface for the fiber optic sensor. The strain signals were directly recorded by a computer. The electro-actuation strains in both the cathode and anode were characterized. The ionic electroactuators of A-aMEGO/polymer nano-composites with pure IL [BMIM][BF_4] were also studied. The capacitance of the ionic A-aMEGO/polymer nano-composite actuators was measured with a potentionstat (Versastat 4, Princeton Applied Research).

Supporting Information

Supporting Information is available from the Wiley Online Library or from the author.

Acknowledgements

The authors wish to thank Zhigang Suo for discussions. The work at Penn State was supported by NSF under grant number CMMI-1130437(MG and WK), AFOSR under grant number FA9550–11–1–0192 (YZ, ML and QMZ), and the Electrical Engineering Department of the Penn State University (QB). SM and RSR appreciate support by the US Department of Energy (DOE) under Award no. DE-SC001951.

Received: March 26, 2013
Revised: July 15, 2013
Published online:

[1] Y. Bar-Cohen, Q. M. Zhang, *MRS Bullet.* **2008**, *33*, 173.
[2] Q. M. Zhang, V. Bharti, X. Zhao, *Science.* **1998**, *280*, 2101.
[3] R. Perline, R. Kornbluh, Q. Pei, J. Joseph, *Science.* **2000**, *287*, 836.
[4] W. Lu, A. G. Fadeev, B. Qi, E. Smela, B. R. Mattes, J. Ding, G. M. Spinks, J. Mazurkiewicz, D. Zhou, G. G. Wallace, D. R. MacFarlane, S. A. Forsyth, M. Forsyth, *Science.* **2002**, *297*, 983.
[5] M. Shahinpoor, Y. Bar-Cohen, J. O. Simpson, J. Smith, *Smart Mater. Struct.* **1998**, *7*, R15.
[6] R. H. Baughman1, C. Cui1, A. A. Zakhidov, Z. Iqbal, J. N. Barisci, G. M. Spinks, G. G. Wallace, A. Mazzoldi, D. De Rossi, A. G. Rinzler, O. Jaschinski, S. Roth, M. Kertesz, *Science.* **1999**, *284*, 1340.
[7] S. Liu, Y. Liu, H. Cebeci, R. Guzmán de Villoria, J. H. Lin, B. L. Wardle, Q. M. Zhang, *Adv. Funct. Mater.* **2010**, *20*, 3266.
[8] T. Thorsen, S. J. Maerkl, S. R. Quarke, *Science.* **2002**, *298*, 580.
[9] M. D. Lima, N. Li, M. J. de Andrade, S. Fang, J. Oh, G. M. Spinks, M. E. Kozlov, C. S. Haines, D. Suh, J. Foroughi, S. J. Kim, Y. Chen, T. Ware, M. K. Shin, L. D. Machado, A. F. Fonseca, J. D. W. Madden, W. E. Voit, D. S. Galvão, R. H. Baughman, *Science.* **2012**, *338*, 928.
[10] M. D. Bennett, D. J. Leo, *Sens. Actuators A.* **2004**, *115*, 79.
[11] J. D. Madden, N. A. Vandesteeg, P. A. Anquetil, P. G. A. Madden, A. Takshi, R. Z. Pytel, S. R. Lafontaine, P. A. Wieringa, I. W. Hunter, *IEEE J. Oceanic Eng.* **2004**, *29*, 706.
[12] Q. M. Zhang, H. Li, M. Poh, F. Xia, Z. Y. Cheng, H. Xu, C. Huang, *Nature.* **2002**, *419*, 284.
[13] P. Calvert, *MRS Bullet.* **2008**, *33*, 207.
[14] M. Knoblauch, G. A. Noll, T. Müller, D. Prüfer, I. Schneider-Hüther, D. Scharner, A. J. E. V. Bel, W. S. Peters, *Nat. Mater.* **2003**, *2*, 600.
[15] D. J. Beebe, J. S. Moore, J. M. Bauer, Q. Yu, R. H. Liu, C. Devadoss, B. H. Jo, *Nature.* **2000**, *404*, 588.
[16] X. Xie, Q. Liangti, C. Zhou, Y. Li, J. Zhu, H. Bai, G. Shi, L. Dai, *ACS Nano.* **2010**, *4*, 6050.
[17] S. Zhu, R. Shabani, J. Rho, Y. Kim, B. H. Hong, J. H. Ahn, H. J. Cho, *Nano. Lett.* **2011**, *11*, 977.
[18] P. Liu, C. G. Massey, G. P. McKnight, W. Barvosa-Carter, G. Herrera, US Patent 7, *205*, 699 B1, **2007**.
[19] Y. Zhu, S. Murali, M. D. Stoller, K. J. Ganesh, W. Cai, P. J. Ferreira, A. Pirkle, R. M. Wallace, K. A. Cychosz, M. Thommes, D. Su, E. A. Stach, R. S. Ruoff, *Science.* **2011**, *332*, 1537.
[20] Q. Liang, X. Yao, W. Wang, Y. Liu, C. P. Wong, *ACS Nano.* **2011**, *5*, 2392.
[21] K. W. Putz, O. C. Compton, C. Segar, Z. An, S. T. Nguyen, L. C. Brinson, *ACS Nano.* **2011**, *5*, 6601.
[22] K. W. Putz, O. C. Compton, M. J. Palmeri, S. T. Nguyen, L. C. Brinson, *Adv. Funct. Mater.* **2010**, *20*, 3322.
[23] D. A. Dikin, S. Stankovich, E. J. Zimney, R. D. Piner, G. H. B. Dommett, G. Evmenenko, S. T. Nguyen, R. S. Ruoff, *Nature.* **2007**, *448*, 457.
[24] B. E. Conway, *Electrochemical Supercapacitors: Scientific Fundamentals and Technological Applications*, Plenum Publishers, New York, **1999**.
[25] Y. Liu, R. Zhao, M. Ghaffari, J. Lin, S. Liu, H. Cebeci, R. Guzmán de Villoria, R. Montazami, D. Wang, B. L. Wardle, J. R. Heflin, Q. M. Zhang, *Sensor. Actuat. A-Phys.* **2012**, *181*, 70.
[26] S. Liu, W. Liu, Y. Liu, J. Lin, X. Zhou, M. J. Janik, R. H. Colby, Q. M. Zhang, *Polym. Intern.* **2010**, *59*, 321.
[27] A. Jarosik, S. R. Krajewski, A. Lewandowski, P. Radzimski, *J. Molec. Liq.* **2006**, *123*, 43.
[28] J. M. Herbert, *Ferroelectric Transducers and Sensors*, Vol. *3*, Gordon and Breach Science Publishers, New York, **1982**.
[29] R. E. Newnham, D. P. Skinner, L. E. Cross, *Mat. Res. Bull.* **1978**, *13*, 525.
[30] P. W. Ruch, R. Kötz, A. Wokaun, *Electrochim Acta* **2009**, *54*, 4451.
[31] J. Foroughi, G. M. Spinks, G. G. Wallace, J. Oh, M. E. Kozlov, S. Fang, T. Mirfakhrai, J. D. W. Madden, M. K. Shin, S. J. Kim, R. H. Baughman, *Science* **2011**, *334*, 494.
[32] Y. Liu, C. Lu, S. Twigg, M. Ghaffari, J. Lin, N. Winograd, Q. M. Zhang, *Sci. Rep.* **2013**, *3*, 973.
[33] V. Giurgiutiu, C. J. Rogers, *Intell. Mater. Syst. Struct.* **1996**, *7*, 656.
[34] D. Maugis, *Contact, Adhesion and Rupture of Elastic Solid*, Springer, New York, **2000**.
[35] O. Sahin, N. Erina, *Nanotechnology.* **2008**, *19*, 445717.
[36] Y. Liu, M. Ghaffari, R. Zhao, J. Lin, M. Lin, Q. M. Zhang, *Macromolecules.* **2012**, *45*, 5128.
[37] X. Zhou, X. Zhao, Z. Suo, C. Zou, J. Runt, S. Liu, S. Zhang, Q. M. Zhang, *Appl. Phys. Lett.* **2009**, *94*, 16290.
[38] Y. Osada, M. Hasebe, *Chem. Lett.* **1985**, 1285.
[39] E. Smela, N. Gadegaard, *Adv. Mater.* **1999**, *11*, 953.
[40] S. Hara, T. Zama, W. Takashima, K. Kaneto, *Smart Mater. Struct.* **2005**, *14*, 1501.
[41] G. M. Spinks, G. G. Wallace, L. S. Fifield, L. R. Dalton, A. Mazzoldi, D. De Rossi, I. I. Khayrullin, R. H. Baughman, *Adv. Mater.* **2002**, *14*, 1728.
[42] M. Hahn, O. Barbieri, R. Gallay, R. Kotz, *Carbon* **2006**, *44*, 2523.
[43] M. Kaneko, K. Kaneto, *Synth. Met.* **1999**, *102*, 1350.